# Thermal Analysis of Trace Levels of Polymorphic Impurity in Salmeterol Xinafoate Samples

**Henry H. Y. Tong,[1] Boris Yu. Shekunov,[2] Peter York,[3] and Albert H. L. Chow[1,4]**

*Received May 22, 2003; accepted May 27, 2003*

***Purpose.*** To quantify trace levels of polymorphic impurity in two salmeterol xinafoate (SX) Form I samples: granular SX (GSX) produced by fast-cooling crystallization and micronized SX (MSX) prepared from GSX by micronization.

***Methods.*** SX-I and SX-II produced by solution enhanced dispersion by supercritical fluids (SEDS™) were the reference polymorphs (100% pure) used for quantitative comparison. The percentage of polymorphic conversion, α, of each Form I sample to Form II was measured by differential scanning calorimetry (DSC) as a function of time (i.e., at different scanning speeds). The data were analyzed by the Avrami-Erofe'ev (AE) equation using an iterative fitting computer program. SX-I samples containing 1.24, 4.41, and 13.47% (w/w) of SX-II as physical mixtures were subjected to similar analysis and data treatment. A mathematical relationship based on an instantaneous nucleation model was derived to relate the AE rate constants, *k*, of pure SX-I and physical mixtures to weight percentage of SX-II. This relationship was then used to calculate the percentage polymorphic impurity of GSX and MSX from their *k* values. For relative comparison of the Form-II nuclei present, the *k* values of SX-I, GSX, and MSX were used to calculate their differences in free energy of nucleation.

***Results.*** The AE equation affords good ($r^2 \approx 0.81$) to excellent ($r^2 \approx 0.99$) fits of data for the samples. The levels of polymorphic impurity in GSX and MSX are 0.16 and 0.62% (w/w), respectively. Based on the free energy differences of nucleation between the reference SX-I material and the other samples, the number (and size) of the Form II nuclei present in the samples rank in the order: MSX > GSX > SX-I.

***Conclusions.*** DSC is a useful tool for assessing the polymorphic purity of SX materials and possibly other enantiotropic pairs showing similar thermal behavior.

**KEY WORDS:** thermal analysis; nucleation model; polymorphic impurity determination; salmeterol xinafoate.

## INTRODUCTION

Polymorphic purity of solid drug substances is an important parameter for consideration in pharmaceutical formulation. Because different polymorphs or crystalline forms of the same drug exhibit different physical properties, chemical stability, solubility, dissolution rate, and possibly bioavailability, the presence of the alternative (metastable) crystal form(s) may have an adverse impact on the manufacturing and *in vivo* performance of the drug product.

A polymorphic impurity or contaminant is prone to form if the polymorphic transition temperature can be readily attained under ordinary conditions. The polymorphic conversion could arise during the batch crystallization process when a local rise in temperature causes the transition temperature to be exceeded momentarily, resulting in partial formation of the alternative crystal form. It could also be induced by subsequent processing treatments such as grinding or milling that generate sufficient heat to cause the temperature to rise above the transition point. In addition to the temperature factor, the presence of trace polymorphic impurity (in embryo or nucleus form) can greatly accelerate the conversion process by lowering the associated activation energy barrier. Regulatory authorities have long recognized the need for limiting polymorphic impurities in pharmaceutical materials. However, the analytic tools available for solid-state characterization, e.g., powder X-ray diffraction (PXRD) and differential scanning calorimetry (DSC), normally do not lend themselves to the quantification of low level (<5%) of polymorphic impurity because of their low sensitivity. Thus, the search for a more sensitive technique for such quantification remains a challenge to formulation scientists.

Previous characterization studies employing DSC have demonstrated that salmeterol xinafoate (SX), a long acting antiasthmatic drug, exists in two enantiotropic polymorphic forms (I and II), as evidenced by melting of Form I (~122.7°C) followed by immediate recrystallization and subsequent melting of Form II at a higher temperature (~137.6°C) (1–3; Fig. 1). The expected polymorphic transition in the solid state at ~99°C (estimated by solubility measurements) could not be observed without vigorous grinding treatment, which had been ascribed to the presence of a relatively high activation energy barrier against the transition (3). The two polymorphs could be prepared in individual pure physical forms by the SEDS™ (Solution Enhanced Dispersion by Supercritical Fluids) crystallization technique. The SEDS™-processed Form I (SX-I) underwent very little conversion to its alternative Form II through recrystallization from its melt, as suggested by the appearance of a relatively small melting endotherm of Form II at 137.6°C (Fig. 1). In contrast, a granular SX material (GSX) of the same Form I structure produced by rapid-cooling crystallization and a micronized SX sample (MSX) prepared from GSX by micronization underwent much more rapid transformation to Form II. The latter was substantiated by the occurrence of a large recrystallization peak immediately after the melting endotherm of Form I at 122.7°C, followed by a large melting endotherm of Form II at 137.6°C. Despite the observed differences in thermal behavior, all three SX samples, i.e., GSX, MSX, and SX-I, exhibited essentially the same powder X-ray diffraction pattern, solid state $^{13}C$ NMR/CP-MAS spectrum, FTIR spectrum, and solubility-temperature dependence. All of these observations suggest that the SEDS™-processed SX-I is much less prone to polymorphic conversion than are Form I samples prepared by conventional methods, which can be attributed to its relative freedom from trace Form II nuclei.

The objective of the present communication was to use DSC to demonstrate quantitatively trace polymorphic impu-

[1] School of Pharmacy, The Chinese University of Hong Kong, Shatin, N.T., Hong Kong SAR, China.
[2] Ferro Corporation, Pharmaceutical Technologies, Independence, Ohio 44131.
[3] Drug Delivery Group, School of Pharmacy, University of Bradford, Bradford BD7 1DP, United Kingdom.
[4] To whom correspondence should be addressed. (e-mail: albert-chow@cuhk.edu.hk)


0724-8741/03/0900-1423/0 © 2003 Plenum Publishing Corporation

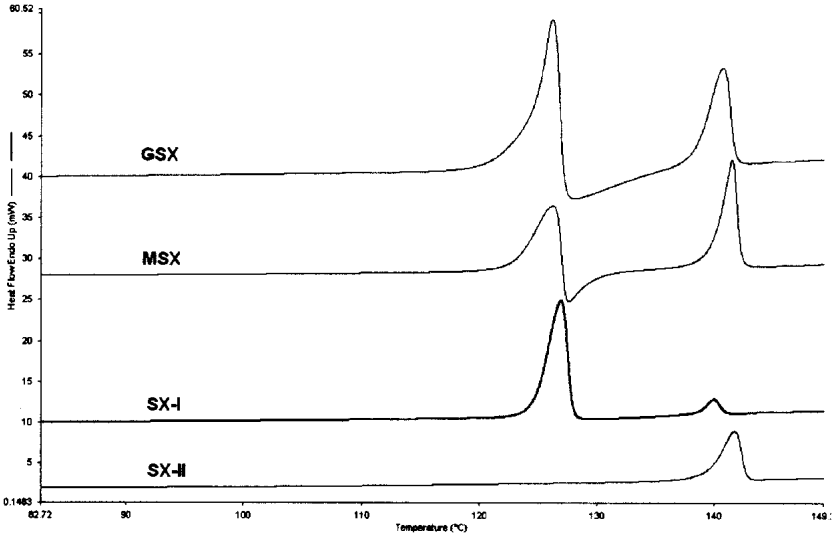


**Fig. 1.** DSC profiles of GSX, MSX, SX-I, and SX-II at 10ºC $min^{-1}$.

rity arising from the batch crystallization process and subsequent processing treatments in the aforementioned SX samples (GSX and MSX). To this end, the SEDS™-processed Form I (SX-I) and Form II (SX-II) materials were used as reference standards for the quantitative analysis.

## MATERIALS AND METHODS

### Chemicals and Reagents

Granular salmeterol xinafoate (GSX) and micronized salmeterol xinafoate (MSX) were generous donations from GlaxoWellcome, Ware, UK. The two pure polymorphic standards for Form I (SX-I) and Form II (SX-II) were prepared by the SEDS™ process as described previously (1). Physical mixtures of SX-I and SX-II were prepared by gentle blending using a geometric dilution technique. Pure SX-I form was subjected to the same mixing process to check for possible generation of Form II nuclei during mixing, and no significant changes in thermal behavior of the pure sample were observed afterwards.

### Thermogravimetric Analysis

Thermogravimetric analysis (TGA) was performed in an open pan using a Perkin Elmer Thermogravimetric Analyzer TGA 7 with Thermal Analysis Controller TAC 7/DX. Approximately 5 mg of sample (accurately weighed) was placed on the pan and scanned at 2 and 10°C $min^{-1}$ from 50 to 250°C.

### Differential Scanning Calorimetry and Dynamic Differential Scanning Calorimetry

Differential scanning calirimetry (DSC) analysis was performed using a Perkin Elmer Pyris 1 differential scanning calorimeter (with Pyris Manager software). Indium ($T_m$ = 156.6°C; $\Delta H_f$ = 28.45 J $g^{-1}$) was used for calibration. Accurately weighed samples (1.5–2.0 mg) were placed in hermetically sealed aluminum pans and scanned at 2 to 100°C $min^{-1}$ under nitrogen purge. All DSC measurements were done in triplicate.

Dynamic differential scanning calorimetry (DDSC) (equivalent of modulated temperature DSC or MTDSC) analysis was conducted using the same DSC equipment as before, together with the DDSC Repeated Scan software. The scanning program was set as follows: heat/cool (90–94°C/94–92°C × 35 cycles); scanning range: 90–160°C. The corresponding linear scanning rate was 5°C $min^{-1}$.

## RESULTS

### Construction of α-Time Curves by DSC at Varying Scanning Speeds

For all DSC scans, recrystallization into Form II was assumed to occur only between the onsets of melting of Form I and Form II. The expected polymorphic conversion at the estimated transition temperature (~99°C) could not be observed even at the lowest scanning speed used, i.e., 2°C $min^{-1}$, probably because of the presence of a high activation energy barrier against the solid–solid conversion (1). Assuming that the temperature range of recrystallization, ΔT, is constant, the time allowed for the recrystallization, $t$, can be calculated from

$$\Delta T = \beta \times t \quad (1)$$

where β is the scanning speed.

Equation (1) shows that $t$ is inversely related to β provided that ΔT remains constant. Although the onsets of the melting endotherms of both SX-I and SX-II tended to shift downward to lower temperature with decreasing scanning speed, the shift was small, and the ΔT remained essentially the same (15.6 ± 0.8°C; n = 84) at all scanning speeds and for all SX samples studied.

TGA data showed that degradation was not apparent within the temperature range of interest at all scanning speeds studied (down to 2°C $min^{-1}$). The $\Delta H_f$ of the second peak (endotherm of Form II) obtained at each scanning speed for GSX, MSX, and SX-I samples was normalized by that of the reference SEDS™-processed Form II (SX-II) sample measured at the same scanning speed to yield the fraction of

material recrystallized, α. The data are presented as α–time curves in Fig. 2.

### Determination of Polymorphic Purity of SX Samples from Quantitative Phase Analysis and Nucleation Model

The α–time curve data of GSX, MSX, and SX-I were fitted to the popular Johnson-Mehl-Avrami-Kolmogorov (JMAK) equation. This model considers crystallization reactions to occur via a process of nucleation and growth:

$$[-\ln(1-\alpha)]^{1/n} = k(t - t_0) \quad (2)$$

where α is the fraction of recrystallized material; $k$ is the crystallization rate constant; $t$ is the crystallization time; $t_0$ is the induction time; and n is the model exponent, normally an integer between 0 and 3, denoting zero-, one-, two-, and three-dimensional nucleation and growth (4). The fitted parameters of the equation are summarized in Table I.

Although all curves showed excellent fit to the JMAK equation ($R^2 > 0.99$), the parameter estimate of the induction time, $t_0$, showed significant variability for all tested samples, as suggested by the relatively high standard errors of the fitted parameters. In addition, the $t_0$ values were statistically indistinguishable for all the samples and were negligible relative to the overall crystallization period. The constant $t_0$ term was therefore omitted from Eq. (2) in the subsequent analysis, yielding Eq. (3) below:

$$[-\ln(1-\alpha)]^{1/n} = k\,t \quad (3)$$

Equation (3) is the well-known classic Avrami-Erofe'ev (AE) rate equation. The α–time curves and the fitted parameters of the equation are shown in Fig. 2 and Table II, respectively. Subtle differences in the mechanisms of nucleation and crystal growth among the samples could be revealed through comparison of the n and $k$ values. It should be noted that the n values are close to 2, which is expected from the fact that SX particles have a platelet shape and therefore predominantly grow in two dimensions (5).

Here we assume the model of instantaneous nucleation, which is characterized by its extremely rapid onset and consistent with its relatively small n value (≈2) (5). Both homogeneous and heterogeneous nucleation can proceed simultaneously. However, homogeneous nucleation can occur only in the bulk material of molten SX-I, whereas heterogeneous nucleation is initiated by contact with the surface of the SX-II seeds present. The number of nuclei formed by heterogeneous nucleation is proportional to the surface area of the metastable phase and will be proportional to the weight fraction of SX-II, $x$, if the same specific surface area is assumed for both preexisting nuclei and SX-II particles added (as in physical mixtures). Therefore, the total number of nuclei, $N_T$, formed at $x << 1$ can be expressed by:

$$N_T = (1-x)N_{HON} + xN_{HEN} \quad (4)$$

where $N_{HON}$ and $N_{HEN}$ correspond to the number of nuclei formed per mole (or unit weight) of melt for homogeneous and heterogeneous nucleation, respectively.

In order to quantify the amount of preexisting nuclei in GSX and MSX, it will be necessary to find a suitable mathematical relationship that relates the (total) rate constant, $k$, which is determined by the AE model-fitting procedure, to the mole fraction of SX-II. The relationship below follows from the instantaneous nucleation model (5):

$$k = (c_g N_T/\Omega)^{1/n} G_c \quad (5)$$

where Ω is the specific molar volume, $c_g$ is the shape factor of SX crystal, and $G_c$ is the growth constant. Manipulation of Eqs. (4) and (5) results in the following expression for $k$:

$$k = [C_1(1-x) + C_2 x]^{1/n} \quad (6)$$

where $C_1$ and $C_2$ are constants related to the homogeneous and heterogeneous contributions, respectively. It should be noted that some other nucleation models, for example, progressive nucleation (5), will also give a relationship similar to Eq. (6) but with different coefficients.

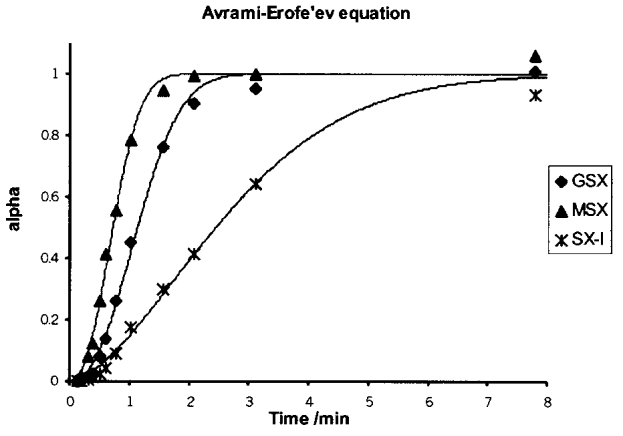


**Fig. 2.** α–time curves of GSX, MSX, and SX-I fitted by the Avrami-Erofe'ev rate equation.

**Table I.** Parameters of the α–Time Curves Fitted by Johnson-Mehl-Avrami-Kolmogorov (JMAK) Rate Equation for the GSX, MSX, and SX-I Samples: $[-\ln(1-\alpha)]^{1/n} = k(t - t_0)$

| | GSX (SD) | MSX (SD) | SX-I (SD) |
|---|---|---|---|
| $k$ ($min^{-1}$) | 0.848 | 1.437 | 0.339 |
| | (0.075) | (0.139) | (0.016) |
| n | 1.938 | 1.739 | 1.466 |
| | (0.240) | (0.249) | (0.160) |
| $t_0$ (min) | 0.156 | 0.156 | 0.156 |
| | (0.094) | (0.063) | (0.126) |
| $r^2$ | 0.998 | 0.997 | 0.996 |

**Table II.** Parameters of the α–Time Curves Fitted by Avrami-Erofe'ev Rate Equation for the GSX, MSX, and SX-I Samples: $[-\ln(1-\alpha)]^{1/n} = kt$

| | GSX (SD) | MSX (SD) | SX-I (SD) |
|---|---|---|---|
| $k$ ($min^{-1}$) | 0.746 | 1.171 | 0.327 |
| | (0.016) | (0.024) | (0.011) |
| n | 2.330 | 2.341 | 1.657 |
| | (0.119) | (0.137) | (0.100) |
| $r^2$ | 0.996 | 0.996 | 0.994 |

It is a common practice to estimate individual polymorphic composition with reference to a calibration curve obtained using physical mixtures of varying polymorphic composition. Accordingly, 1.24, 4.41, and 13.47% (w/w) SX-II in SX-I were prepared, and the α–time curves constructed as described before. For GSX, MSX, and SX-I, excellent reproducibility, with standard deviation of less than 5%, was observed for all data points. However, data variability with the physical mixtures appeared to be much larger than that with individual GSX, MSX, and SX-I samples. This is probably caused by nonhomogeneous mixing, a problem not uncommon with blending of powders in widely different proportions. In order to account for all experimental errors in the final statistical analysis, individual data points instead of the average values obtained at each defined scanning rate were fitted to the AE equation. The fitted parameters for the physical mixtures of SX-I and SX-II are tabulated in Table III.

It is interesting to note that the fitted n values for the physical mixtures remain essentially constant at different levels of SX-II, being close to 2 (i.e., two-dimensional growth) (see Table III). Therefore, the data were refitted to the AE equation by keeping n = 2 for all the samples (including MSX and GSX) so as to standardize the calculation of polymorphic composition from respective *k* values [see Eq. (7) below]. The fitted parameters are shown in Table IV, and the rate constants at different weight percentages of SX-II are presented in Fig. 3.

Equation (6) was used to fit the rate constant data for the physical mixtures of SX-I and SX-II. With n fixed as 2, good data fitting was obtained.

$$k = [0.257 \pm 0.406\,(1 - x) + 167 \pm 25.4\,x]^{1/2}$$
$$r^2 = 0.967 \qquad (7)$$

Equation (7) was used to construct a calibration curve for different weight proportions of SX-I and SX-II, as shown in Fig. 3. The proportions of phase II in GSX and MSX can be calculated from their respective n and *k* values. With n = 2, GSX and MSX were found to contain 0.16% and 0.62% (w/w) of metastable nuclei within their crystal matrices.

### Relative Comparison of Polymorphic Purity of SX Samples Based on Differences in Free Energy of Nucleation

A second approach for comparing polymorphic purity can be formulated using the concept of free energy of nucleation for different samples. Thus, the rate of nucleation, *J*, can be expressed in the form of Arrhenius' rate equation:

**Table III.** Parameters of the α–Time Curves Fitted by Avrai-Erofe'ev Rate Equation for Physical Mixtures of SX-I and SX-II: $[-1n\,(1 - \alpha)]^{1/n} = kt$

| | 0.00% of SX-II in SX-I (SD) | 1.24% of SX-II in SX-I (SD) | 4.41% of SX-II in SX-I (SD) | 13.47% of SX-II in SX-I (SD) |
|---|---|---|---|---|
| $k$ ($min^{-1}$) | 0.327 (0.011) | 2.026 (0.100) | 2.640 (0.164) | 4.651 (0.304) |
| n | 1.657 (0.100) | 1.756 (0.206) | 1.498 (0.217) | 1.637 (0.340) |
| $r^2$ | 0.994 | 0.935 | 0.869 | 0.801 |

**Table IV.** Parameters of the α–Time Curves Fitted by Avrami-Erofe'ev Rate Equation with n (Fixed at 2 for All Samples: $[-\ln\,(1 - \alpha)]^{1/2} = kt$

| | $k$ ($min^{-1}$) (SD) | $r^2$ |
|---|---|---|
| 0.00% of SX-II in SX-I (pure SX-I) | 0.348 (0.011) | 0.990 |
| 1.24% of SX-II in SX-I | 2.072 (0.087) | 0.937 |
| 4.41% of SX-II in SX-I | 2.700 (0.144) | 0.877 |
| 13.47% of SX-II in SX-I | 4.645 (0.265) | 0.820 |
| GSX | 0.724 (0.020) | 0.992 |
| MSX | 1.135 (0.029) | 0.993 |

$$J = A \exp(-\Delta G/k_B T) \qquad (8)$$

where $A$ is the frequency factor; $\Delta G$ is the excess free energy of nucleation; and $k_B$ is the Boltzmann constant. $\Delta G$ is a function of the overcooling, $\Delta T/T$, and also depends on the surface excess free energy between the surface of the crystallizing solid and the bulk of the solid. $\Delta G$ of nuclei formed in the presence of existing Form II phase is significantly reduced because the homogeneous nucleation mechanism in the pure melt changes over to the heterogeneous nucleation mechanism on initiation by the solid phase II.

Based on the concept of a lowering of the free-energy barrier for the whole sample bulk, the effect of preexisting embryos or nuclei should be much more pronounced on the exponential $\Delta G$ term than on the preexponential $A$ term, i.e., the change in $A$ among the three tested samples should be small compared with that in $\Delta G$. This assumption can be justified on the basis that in pure melt, the $A$ term is defined by the rate of attachment and rearrangement of molecules from the melt into the crystal lattice, which in turn is governed by the activation energy involved (6). Therefore, the coefficient $A$ should depend mainly on the temperature and properties of melt (density and viscosity) and should be less af-

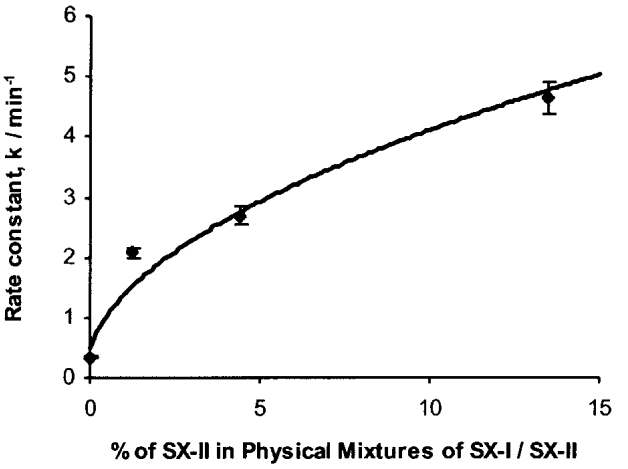


**Fig. 3.** Relationship of weight percentage of SX-II and *k* values in the Avrami-Erofe'ev equation with n = 2.

fected by the presence of the preexisting embryos. For the instantaneous nucleation model being considered, the number of nuclei formed, $N_T$, is proportional to the rate of nucleation, $J$ (5):

$$J = (N_T/\Omega)\,\delta(t) \tag{9}$$

where $\delta(t)$ is the Dirac delta function, which defines the instantaneous character of nucleation. Thus, for comparison of the free energy of nucleation between two samples, the following equation can be derived from Eqs. (5), (8), and (9):

$$\ln (k_2^{n2}/k_1^{n1}) = (\Delta G_1 - \Delta G_2)/RT \tag{10}$$

where R is the gas constant; $k_1$, $k_2$, and n1, n2 are the rate constants and nucleation orders for two different samples. If $k$, n, and T are known, the difference in free energy of nucleation, $\Delta G_1 - \Delta G_2$ (kJ mol$^{-1}$) between two SX samples (e.g., GSX and SX-I) can be determined.

In the present calculation, T was taken as the peak recrystallization temperature, which was determined by DDSC, as described in the Materials and Methods section. The DOSC or MTDSC heat flow and resolved storage Cp and loss Cp curves of MSX are depicted in Fig. 4. The exothermic peak at ~126°C in the loss Cp curve indicated the recrystallization of Form I melt. The recrystallization peak temperatures of GSX, MSX, and SX-I were relatively constant, being 126.4°C, 125.2°C, and 126.6°C, respectively. Thus, a mean T value of 126.1°C was used to calculate the free energy of nucleation.

The calculated free energy of nucleation of SX-I is 4.86 kJ mol$^{-1}$ and 7.85 kJ mol$^{-1}$ higher than those of GSX and MSX, respectively, whereas the free energy of nucleation of GSX is 2.98 kJ mol$^{-1}$ higher than that of MSX. Thus, the order of free energy of nucleation is SX-I > GSX > MSX. Hence, the size or concentration of metastable nuclei is in the order of MSX > GSX > SX-I (see Discussion).

## DISCUSSION

### Avrami-Erofe'ev Rate Equation

The pharmaceutical applications of the Avrami-Erofe'ev (AE) rate equation have been reviewed extensively elsewhere and are not elaborated here (7). In the AE model, the difference in nucleation mechanism could be deduced from

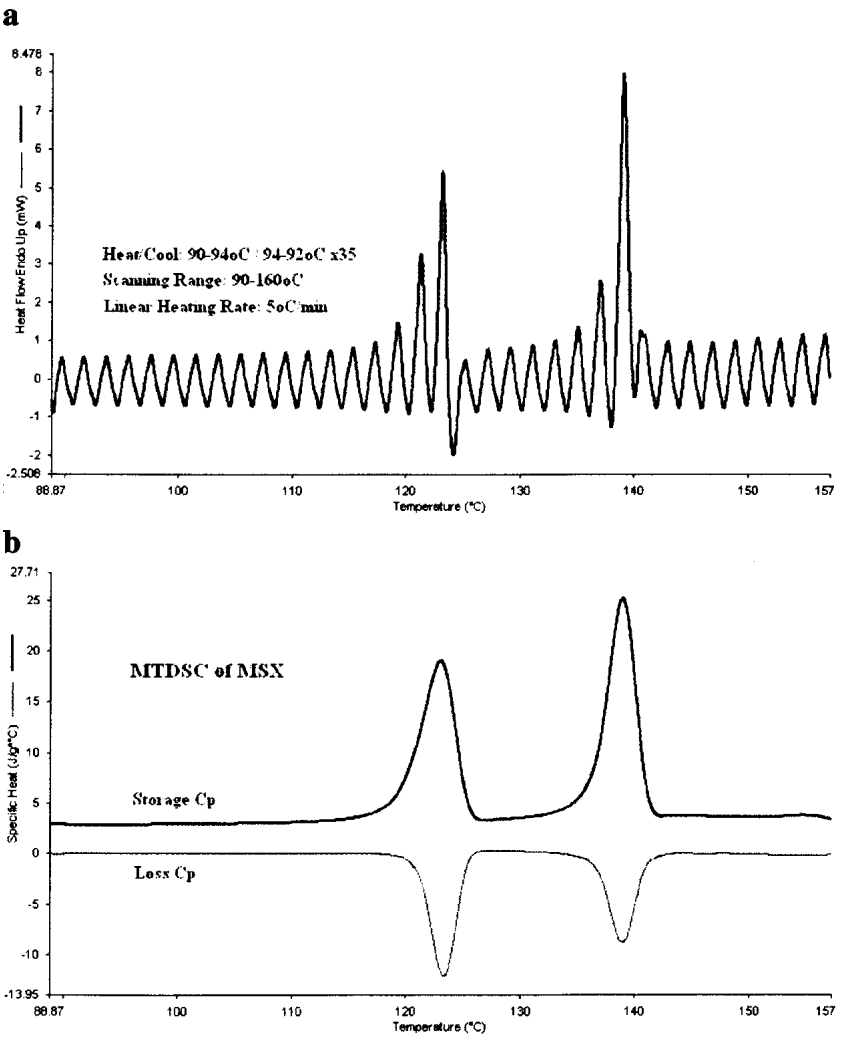


**Fig. 4.** a, Heat flow in MTDSC curve of MSX. b, Storage Cp (reversible heat flow) and loss Cp (irreversible heat flow) deduced from heat flow in MTDSC curve of MSX.

the difference in the nucleation parameter (n) values. The n values of the GSX and MSX samples were found to be statistically equivalent, reflecting similar nucleation mechanism (Table II). On the other hand, the higher value of the growth parameter ($k$) observed for MSX suggests that the MSX melt underwent recrystallization into Form II more readily than did GSX. Compared with GSX and MSX, nucleation and recrystallization of the melt from SX-I occurred less readily, as suggested by its lower n and $k$ values (Table II).

In the present study, GSX, MSX, and SX-I are essentially of the same crystal structure (i.e., Form I). All the thermal events occurred within the confined space of the sealed aluminum pans, and the only factor governing the recrystallization process would be the relative size and number of the Form II preexisting nuclei in all SX samples studied. Because all of these three samples were confirmed by HPLC to have high chemical purity (~99%), the observed differences in recrystallization rate would imply that SX-I had very few, if any, Form II nuclei compared with both GSX and MSX.

As has been documented, GSX is a novel readily micronizable form of SX produced by a patented crystallization method (8). Being friable in nature, GSX can be broken down readily by micronization to yield the micronized form (MSX). Although MSX has a higher recrystallization rate constant, $k$, than GSX, the difference is unlikely to be of stability-related concern because the additional Form II nuclei generated by the micronization process is still well below 1% (0.62% in MSX vs. 0.16% in GSX). This finding serves to illustrate the advantageous aspect of the patented crystallization technology that the crystal structure of GSX was not seriously damaged by the micronization process, which could have generated substantial crystal defects, amorphous solid phases, and nuclei of the metastable form in the drug materials.

### Difference in Free Energy of Nucleation

Equation (8) affords a simple and readily interpretable means to relate the free energy of nucleation to various controlling factors such as nucleus size and interfacial tension, $\gamma$. It has been established through the nucleation theory (5,6,9) that a reduced $\gamma$ and an increased curvature of the foreign surfaces (in this case preexisting phase II nuclei) promote nucleation. Because the nucleation rate constants ($k$) of the samples follow the order: MSX > GSX > SX-I (Table II), the $\Delta G$ should rank in the reverse order, i.e., MSX < GSX < SX-I, which has been confirmed by the calculated differences in free energy of nucleation. Consequently, the order of the number (and size) of the Form II nuclei present in the three samples would be MSX > GSX > SX-I, as based on Eq. (8).

### Quantitative Analysis of Metastable Nuclei in GSX and MSX

In the present analysis, the nucleation mechanisms are considered similar for pure SX-I as well as the various physical mixtures of SX-I and SX-II, as reflected by the n values obtained (see Table III). It can be envisaged that the contribution of heterogeneous nucleation becomes increasingly important as the weight (or mole) proportion of SX-II increases. The equation derived from the instantaneous nucleation model appears to relate well the rate constants, $k$, of the samples to the respective weight proportions of SX-II ($r^2$ = 0.967). However, the fitted homogeneous nucleation coefficient [$C_1$ in Eq. (7)] exhibits substantial variability, as reflected by its large standard error. The statistical uncertainty is largely a result of an insufficient number of data points at the low end of the calibration curve (i.e., the region of interest for trace level quantification), which can compromise the accuracy of the impurity determination.

There is also another potential source of error in the current calculation. In order to standardize the determination of polymorphic impurity from the rate constant, $k$, for all the samples, the n values need to be fixed at 2. Implicit in this approach is the assumption that all the SX samples share the same nucleation mechanism (i.e., two-dimensional growth), which may not be true for the GSX, MSX, and pure SX-I samples because they have different formation and treatment histories. In addition, all the Form I samples are assumed to differ only in the number but not in the size of the nuclei. As alluded to earlier, conventional solid-state characterization methods, such as PXRD, FTIR, and solid state $^{13}C$ NMR with CP/MAS, cannot reveal the presence of Form II nuclei in GSX, MSX, and SX-I because of their low sensitivity (<5%). With SEDS™-processed SX-I used as a pure polymorphic reference material for comparison and DSC as a sensitive tool for monitoring the rate of polymorphic transformation, the amount of metastable nuclei present in the GSX and MSX samples (0.16% and 0.62% w/w) can be readily determined.

## CONCLUSION

The present study clearly demonstrates that trace polymorphic impurity present as Form II nuclei in two industrial salmeterol xinafoate samples can be quantified by DSC from the respective melt recrystallization rate constant, $k$, computed from the Avrami-Erofe'ev rate equation. Qualitative comparison of the number of metastable nuclei present in GSX and MSX can also be made on the basis of the difference in free energy of nucleation between these samples and the pure reference supercritically processed (SX-I) material. The reference material distinctly shows a more superior polymorphic purity than the micronized counterpart. DSC is a useful tool for assessing the polymorphic purity of SX materials and possibly other enantiotropic pairs showing similar thermal behavior.

## ACKNOWLEDGMENTS

This study was supported in part by financial support from the Research Grant Council of Hong Kong (Earmarked Grant CHHK4244/98M).

## REFERENCES

1. H. H. Y. Tong, B. Y. Shekunov, P. York, and A. H. L. Chow. Characterization of two polymorphs of salmeterol xinafoate crystallized from supercritical fluids. *Pharm. Res.* **18**:852–858 (2001).
2. P. York, M. Hanna, and G. O. Humphreys. Crystal engineering and particle design for drug delivery systems using supercritical fluid technologies. *Proceedings of the Asian Conference and Ex-*

*hibition on Controlled Release.* Controlled Release Society, Inc., pp.134-135, 1999.
3. S. Beach, D. Latham, C. Sidgwick, M. Hanna, and P. York. Control of the physical form of salmeterol xinafoate. *Org. Proc. Res. Dev.* **3**:370–376 (1999).
4. C. Michaelsen and M. Dahms. On the determination of nucleation and growth kinetics by calorimetry. *Thermochim. Acta* **288**: 9–27 (1996).
5. D. Kashchiev. *Nucleation: Basic Theory with Applications*, Butterworth-Heinemann, Oxford, 2000.
6. A. A. Chernov. *Modern Crystallography III, Crystal Growth, Springer Series in Solid-State Physics*, Springer, Berlin, 1984.
7. S. R. Byrn, R. R. Pfeiffer, and J. G. Stowell. *Solid State Chemistry of Drugs (2nd ed.),* SSCI Inc, West Lafayette, Indiana, 1999.
8. S. F. Beach, D. W. S. Latham, T. G. Roberts, and C. B. Sidgwick. *Benzenedimethanol suitable for micronization.* United States Patent No. 5,380,922, 1995.
9. J. W. Mullin. *Crystallization (3rd ed.)*, Butterworth-Heinemann, Oxford, 1993.